

# A comparison of experimental and predicted results for laminar natural convection in an enclosure

F. W. Schmidt\*, P. W. Giel\*, R. E. Phillipst and D. F. Wang\*\*

An experimental and numerical study of laminar natural convection in a water-filled enclosure with an aspect ratio of 2:1 was conducted. Two opposing vertical walls were held at different uniform temperatures. The remaining four walls of the enclosure were insulated. The Rayleigh number based upon the height of the enclosure was  $6.4 \times 10^8$  while that based upon the distance between the two isothermal plates was  $8 \times 10^7$ . The mean vertical velocities were measured using a two-beam laser Doppler anemometer system with forward scatter. The mean temperature profiles were obtained using a small, 0.07 mm diameter, chromel-alumel thermocouple probe. A multilevel-multigrid algorithm was used to predict the flow for the experimental conditions studied. The predicted and experimental results for the mean vertical velocity profiles were compared and found to be in excellent agreement.

**Keywords:** *natural convection, numerical methods, heat transfer*

## Introduction

The study of natural convection flows in an enclosure has received considerable attention during the past two decades. A number of review articles has been published<sup>1-3</sup> and these represent an excellent summary of past research activities. In one, Catton<sup>2</sup> summarized the various flow regimes observed in a rectangular cavity. The Rayleigh number used to categorize the flow was based upon the distance between the two isothermal walls.

The most comprehensive experimental study to date was reported by Elder<sup>4,5</sup>. Three fluids were used: medicinal paraffin, silicone oil, and water. The study covered turbulent as well as laminar flows. The mean velocity was measured by suspending aluminium particles in the fluid and using streak photographic techniques. Fine thermocouple probes were used to determine the temperature distribution in the fluid. A limited number of more recent experimental studies has been reported<sup>6-14</sup>. The majority of these are of laminar flow.

A large number of papers has been published describing various numerical techniques applied to the prediction of natural convection flows in an enclosure. In 1979 Ian Jones proposed that a detailed study of buoyancy-driven flows in a square cavity with vertical sides, which are differentially heated, be used as a vehicle

for testing and assessing the efficiency and accuracy of a number of numerical methods. A call for contributions was issued in 1979 and thirty groups responded by submitting 37 contributions. A summary and discussion of the main features of the contributions, and a quantitative comparison between them and the benchmark solution of de Vahl Davis<sup>15</sup>, was presented by de Vahl Davis and Jones in 1983<sup>16</sup>. The calculated flows were all in the laminar flow region. A number of methods proved unable to obtain converged solution at high Rayleigh numbers,  $1 \times 10^9$ .

The objective of this study was to determine experimentally the flow characteristics in an enclosed cavity constructed with one vertical hot isothermal wall located opposite a vertical cold isothermal wall. All the other walls were insulated. In order to test more severely the computational algorithm, the study was conducted at a relatively high Rayleigh number near the upper limit of the laminar flow region. The Rayleigh number based on the height of the enclosure was  $Ra_H = 6.4 \times 10^8 \pm 9\%$  while that based on the distance between the two isothermal plates was  $Ra_L = 8 \times 10^6$ . The slight variation in Rayleigh number was associated with the fact that the data were taken over a time span of weeks, and it was impossible to maintain identical thermal conditions.

## Experimental details

A photograph of the experimental arrangement is shown in Fig 1. Specific details associated with the test cell and instrumentation are described below.

### Test cell

The interior dimensions of the enclosure were: height,

\* Department of Mechanical Engineering, The Pennsylvania State University, University Park, PA 16802, USA

† Department of Mechanical Engineering, University of New Hampshire, Durham, NH, USA

\*\* Department of Mechanical Engineering, University of Illinois, Urbana, IL, USA

Received 4 November 1985 and accepted for publication on 10 February 1986

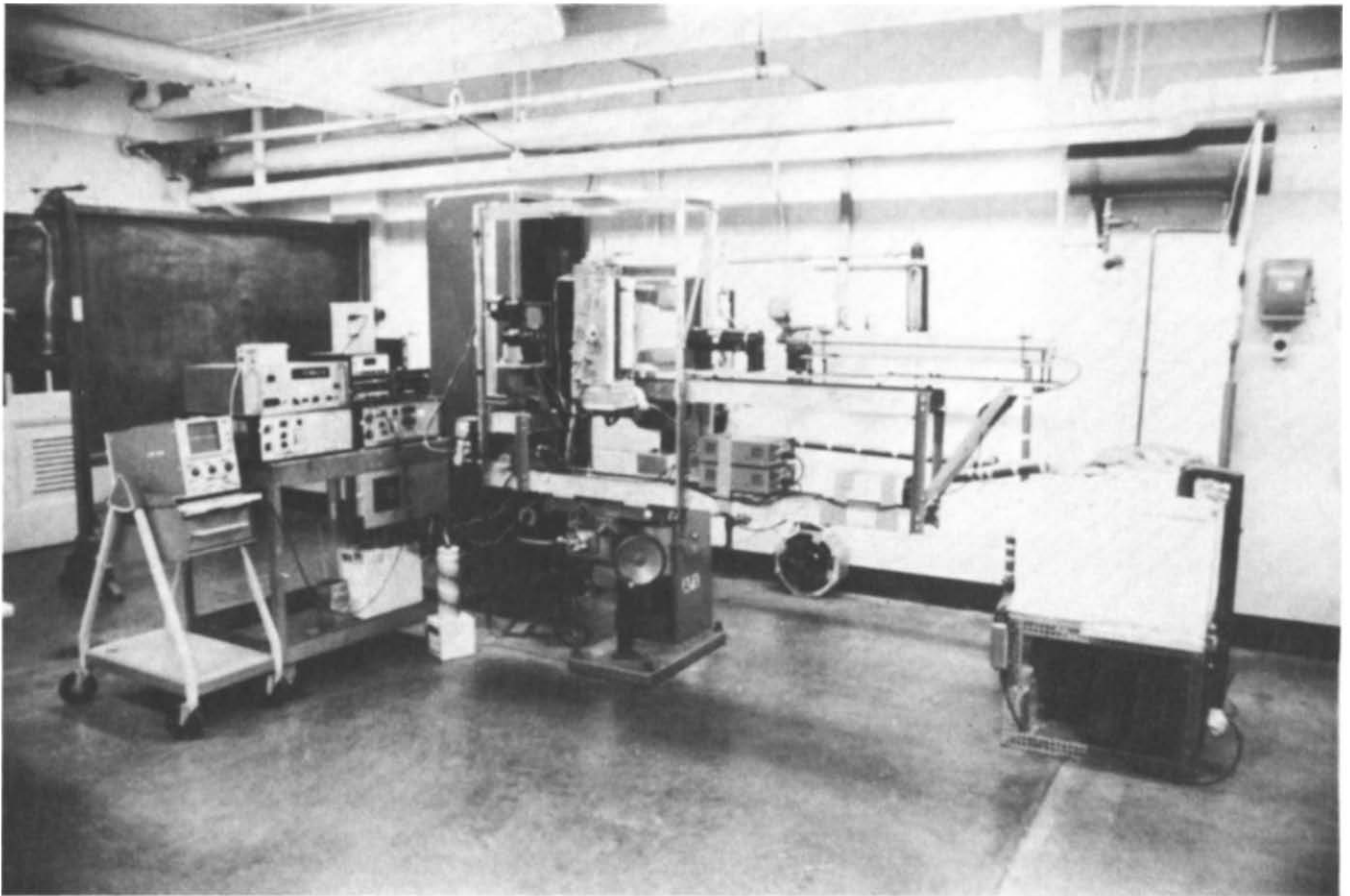


Fig 1 Photograph of test cell and instrumentation

0.386 m; depth, 0.381 m; distance between the hot and cold walls, 0.1905 m. The two ends of the enclosure were Pyrex glass 1.27 cm thick, and the top and bottom of the enclosure were clear acrylic sheets 0.95 cm thick. The hot and cold walls were copper plates 0.95 cm thick. The entire enclosure was insulated with 5 cm expanded polystyrene insulation to reduce heat transfer between the test chamber and the surroundings. A sketch of the cell is

shown in Fig 2. The unit was filled with laboratory grade distilled water.

Ten horizontal heating pads were installed on the outside of one of the copper plates. Each heating pad was connected to a variable power supply to allow independent control of the amount of heat released to the copper plate at each heated section. This was done to obtain a uniform temperature distribution on the interior

Notation			
$D$	Depth of test cell	$t$	Dimensional temperature
$g$	Gravitational acceleration	$t_m$	Mean temperature, $(t_H - t_C)/2$
$Gr_L$	Grashof number, $\frac{g\beta(t_H - t_C)L^3}{\nu^2}$	$U$	Dimensionless $u$ velocity, $u/v_r$
$Gr_H$	Height Grashof number, $\frac{g\beta(t_H - t_C)H^3}{\nu^2}$	$\bar{u}$	Mean velocity in $x$ direction
$H$	Height of test cell	$V$	Dimensionless $v$ velocity, $v/v_r$
$L$	Width of test cell	$v$	Mean velocity in $y$ direction
$P$	Dimensionless pressure, $p/\rho v_r^2$	$v_r$	Characteristic velocity, $\{g\beta(t_H - t_m)L\}^{1/2}$
$p$	Dimensional pressure	$X, Y, Z$	Dimensionless coordinates, $x/L, y/L, z/L$
$Ra_H$	Rayleigh number based on height of enclosure	$x, y, z$	Dimensional coordinates
$Ra_L$	Rayleigh number based on distance between the two isothermal plates	$\beta$	Volumetric thermal expansion coefficient
$T$	Dimensionless temperature, $\frac{t - t_C}{t_H - t_C}$	$\theta$	Dimensionless temperature, $\frac{t - t_m}{t_H - t_m}$
		$\nu$	Kinematic viscosity
		$\rho$	Density
		$T$	Dimensionless time, $\tau v_r/L$
		$\tau$	Dimensional time
		<b>Subscripts</b>	
		C	Cold wall
		H	Hot wall

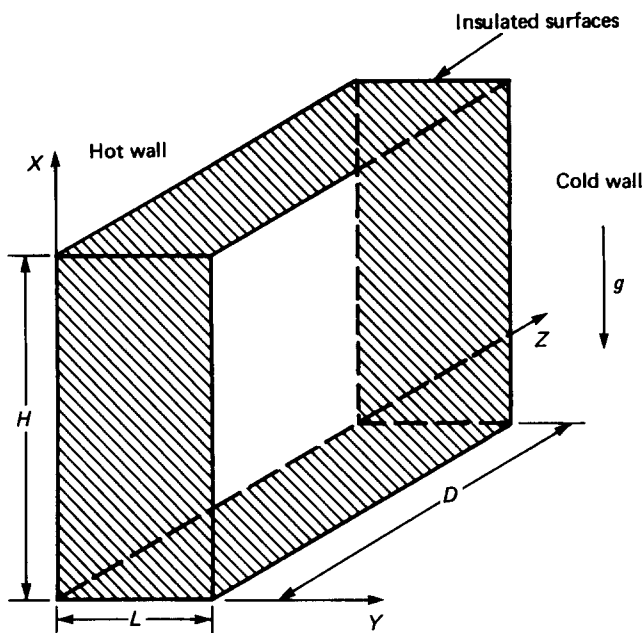


Fig 2 Schematic sketch of enclosure

surface of the hot plate. The surface temperature variation on the hot plate was less than  $\pm 0.11^\circ\text{C}$  ( $\pm 3.4\%$  of the total temperature difference between the hot and cold plates).

Three independent flow channel labyrinths for cooling water were milled in an aluminium plate. This plate was attached to the back of the copper plate and the water was allowed to circulate through the channels in contact with the back of the cold plate. The variation in the surface temperature of the cold plate was less than  $\pm 0.14^\circ\text{C}$  ( $\pm 4.5\%$  of the total temperature difference between the hot and cold plates).

## Instrumentation

### Thermocouples

All wall temperatures were measured by 0.2 mm copper-constantan thermocouples. The temperature profiles in the water were measured with a 0.07 mm (0.003 in) chromel-alumel thermocouple probe. The probe was L-shaped so that its influence on the flow of the fluid in the immediate vicinity of the probe would be minimized. The accuracy of the fluid temperature measurements was estimated to be  $\pm 0.1^\circ\text{C}$ .

### Laser Doppler anemometer

The laser Doppler anemometer (LDA) used a Spectra Physics 15 mW helium-neon laser of 632.8 nm wavelength with forward scatter. A Bragg cell (TSI Model 9180) was used. The accuracy of the velocity measurements was improved by using different shift frequencies depending on the expected magnitude of the velocity component to be measured. The signal was received by a photomultiplier (TSI Model 9160) and processed by a counter (TSI Model 1980 A). The LDA was secured to a long U-shaped optical bench which had the capability of traversing in all three spatial directions with a precision of 0.025 mm (0.001 in).

Different types of seeding were tried. The most

favourable results were obtained by using a very dilute mixture of titanium dioxide powder, mean diameter  $3\ \mu\text{m}$ , and distilled water. Repeatability tests indicated a maximum uncertainty in the mean velocity measurements of  $\pm 0.2\ \text{mm/s}$ .

## Experimental results

A brief flow visualization study was conducted to obtain information on the overall flow patterns present in the enclosure. Several different methods were used, including particle tracing using polystyrene spheres of average diameter  $225\ \mu\text{m}$ , dye tracing and a shadowgraph. These all indicated that the flow was confined to a region adjacent to the walls of the test cell. A schematic sketch of the observed flow patterns is shown in Fig 3. The major portion of the fluid moved up the hot wall, along the top wall to the cold wall, down the cold wall and back along the bottom wall. Two secondary flow recirculation areas were observed: one near the top of the hot wall, while the other was located near the bottom of the cold wall. No fluid motion could be detected in the centre core of the cell or in the Z (crosswise) direction.

The mean vertical velocity and dimensionless temperature profiles are shown in Fig 4. The velocities were measured using the two-beam LDA system described previously. The profiles were obtained at a plane located midway between the front and the back of the test cell,  $Z = 1$ . Velocity profiles were also obtained at  $Z = 1/2$  and  $3/2$  and confirmed that no detectable flow was present in the Z direction, ie the flow was two-dimensional.

Starting at the bottom of the hot wall one can observe that the velocity profiles develop more slowly than, but with the same general trend as, the flow in a fluid adjacent to a vertical hot plate in an infinite cooler fluid.

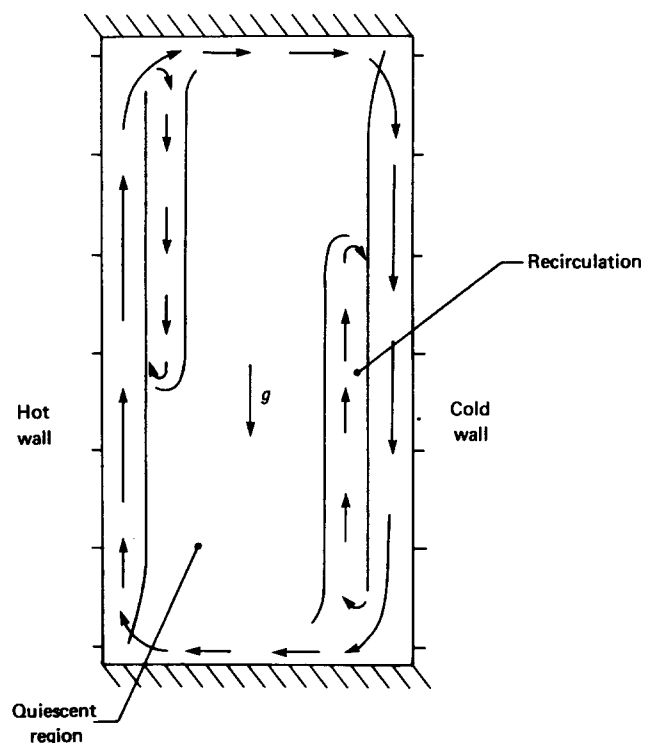


Fig 3 Schematic sketch of flow regions

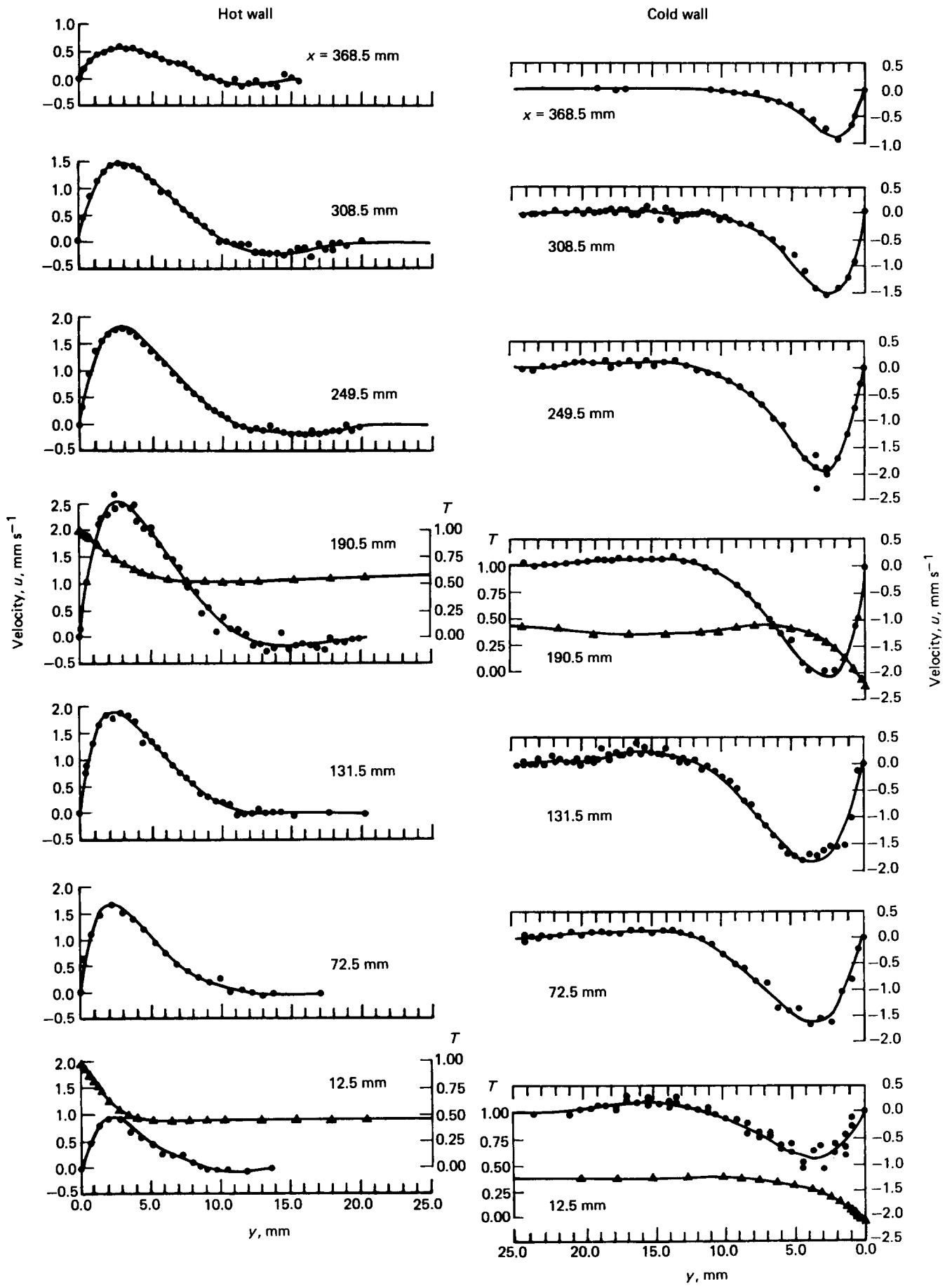


Fig 4 Mean velocity and temperature profiles

**Table 1 Mass flow rate at several horizontal planes**  
*Mass flowrate, kg/ms × 10<sup>3</sup>*

Location	Hot wall			Cold wall			Difference
	Primary flow	Recirculating flow	Net	Primary flow	Recirculating flow	Net	
368.5 mm	3.39	-0.35	3.04	-3.81	0	-3.81	-0.77
308.5 mm	9.20	-1.07	8.13	-8.18	0	-8.18	-0.05
249.5 mm	11.39	-1.01	10.38	-11.22	0.78	-10.44	-0.06
190.5 mm	15.97	-0.97	15.00	-12.67	0.97	-11.7	3.3
131.5 mm	11.48	0	11.48	-12.21	1.57	-10.64	0.84
72.5 mm	9.37	0	9.37	-10.67	1.17	-9.50	-0.13
12.5 mm	4.35	0	4.35	-5.33	1.30	-4.30	0.32

The slower development is associated with the fact that the fluid is thermally stratified in the centre core with a gradient of 4.42°C/m. The magnitude of the source term driving the flow is proportional to the difference in the fluid temperature and that in the centre of the cell at the same elevation. As this temperature difference decreases, the flow decelerates. This can be seen by comparing the mean velocity profiles at  $x=190.5$ , 249.5, 308.5 and 368.5 mm. The converse is true for the flow down the cold wall.

The cell width was 190.5 mm and the centre core, with no measurable vertical mean velocity, was approximately 150 mm in width. The thicknesses of the secondary and primary flow regions, at locations where both were present, were nearly equal.

The dimensionless temperature profiles were measured at two vertical locations,  $x=12.5$  and 190.5 mm. A temperature undershoot was detected at  $x=190.5$  mm in the recirculation regions as indicated by the presence of fluid temperatures less than that in the core along the hot wall or greater than the core temperature along the cold wall. In the analysis of the temperature data it should be noted that the temperature difference between the two isothermal walls was small: 3.2°C. The surface temperature of the hot wall was 9.53°C with a standard deviation of  $\pm 0.11$ °C while that of the cold wall was 6.31°C with a standard deviation of  $\pm 0.14$ °C. A combination of these factors resulted in a slightly negative value for the dimensionless temperature at the cold wall at  $x=190.5$  mm.

Extreme difficulties were encountered when measuring the temperature profiles of the fluid in the test cell. The buoyant forces are relatively small and the maximum velocity is of the order of 2.5 mm/s. The centre core of the fluid is stratified with a temperature slope of 4.42°C/m and no detectable velocity. Any disturbances in the fluid in the outer edge of the boundary layer or the centre core will take a very long time, perhaps days, to die out and return the fluid in the cavity to thermal equilibrium. Although great care was taken, the results obtained were judged to have an accuracy of only  $\pm 0.15$ °C. The combination of relatively small temperature differences, thermocouple errors due to movement of the thermocouple probe during traversing, and the temperature variations on the hot and cold walls, as noted previously, introduced errors of the order of  $\pm 0.1$  in the dimensionless temperature  $T$ .

The mass flow through a horizontal plane was

calculated by integrating the product of the density and mean vertical velocity across the cell. The mass flow rates per unit depth are presented in Table 1. The results indicate agreement within 8% at all locations except at  $x=190.5$  and 368.5 mm, where differences of 25% were present.

The mean horizontal could not be measured since it had a very small magnitude that fell within the error bounds of the velocity measuring system. The mass flow rates in Table 1 indicate a very small (about 0.01 mm/s) horizontal velocity in the upper half of the cell, and an equally small negative velocity in the lower half of the cell at the midplane location between the two isothermal vertical walls.

The transient characteristics of the thermocouple signal were determined at several locations. If temperature fluctuations were present they would most likely appear in the region near the top of the hot wall or near the bottom of the cold wall. A number of strip chart records were taken at various locations in the cell and no detectable temperature fluctuations were measured. This confirms that only laminar flow was present.

### Numerical method

The flow is considered to be two-dimensional and is governed by the following dimensionless equations.

continuity:

$$\frac{\partial U}{\partial X} + \frac{\partial V}{\partial Y} = 0$$

x-momentum:

$$\frac{\partial U}{\partial T} + \frac{\partial(U^2)}{\partial X} + \frac{\partial(UV)}{\partial Y} = \frac{1}{Gr_L^{1/2}} \left( \frac{\partial^2 U}{\partial X^2} + \frac{\partial^2 U}{\partial Y^2} \right) - \frac{\partial P}{\partial X} + \theta$$

y-momentum:

$$\frac{\partial V}{\partial T} + \frac{\partial(UV)}{\partial X} + \frac{\partial(V^2)}{\partial Y} = \frac{1}{Gr_L^{1/2}} \left( \frac{\partial^2 V}{\partial X^2} + \frac{\partial^2 V}{\partial Y^2} \right) - \frac{\partial P}{\partial Y}$$

energy:

$$\frac{\partial \theta}{\partial T} + \frac{\partial(U\theta)}{\partial X} + \frac{\partial(V\theta)}{\partial Y} = \frac{1}{Gr_L^{1/2} Pr} \left( \frac{\partial^2 \theta}{\partial X^2} + \frac{\partial^2 \theta}{\partial Y^2} \right)$$

The boundary conditions are:

$$X = 0, 0 < Y < 1 \quad U = 0, V = 0 \quad \frac{\partial \theta}{\partial X} = 0 \quad \frac{\partial P}{\partial X} = 0$$

$$\begin{aligned}
 X=2, 0 < Y < 1 \quad U=0, V=0 \quad \frac{\partial \theta}{\partial X} = 0 \quad \frac{\partial P}{\partial X} = 0 \\
 0 < X < 2, Y=0 \quad U=0, V=0 \quad t=t_H \quad \frac{\partial P}{\partial Y} = 0 \\
 0 < X < 2, Y=1 \quad U=0, V=0 \quad t=t_C \quad \frac{\partial P}{\partial Y} = 0
 \end{aligned}$$

The appropriate finite difference equations are formed using the QUICK differencing scheme of Leonard. A transient form of the pressure implicit split operator method, PISO, proposed by Issa<sup>17</sup> is used in conjunction with the multilevel-multigrid algorithm developed by Phillips and Schmidt<sup>18</sup>.

The solution of the set of finite difference equations is accomplished by the use of the fast acceleration technique proposed by Brandt<sup>19</sup>. It works on the principle that the computational errors present in the solution of the set of difference equations have a spectral distribution in terms of the wave number:

$$\beta = \frac{P\pi}{Nh}$$

where  $N$  is the number of subdivisions;  $P$  is an index, ie  $P=1,2,3 \dots, N$ ; and  $h$  is the grid spacing. For a given grid pattern there is a range of the spectrum, in the high wave number region, over which the convergence rate of the solution, ie elimination of the high wave number components of the error, is rapid.

The multilevel acceleration technique uses this phenomenon by employing a number of grid patterns with different grid spacing, where each pattern covers the complete region of interest. The coarsest grid will be referred to as level 1 and each successive finer grid will be identified by a larger number. The finest level will be the most efficient in the reduction of the error in the high wave number portion of the error spectrum, while the calculation from the coarsest grid reduces the error in the low wave number region. The solution procedure progresses from level 1 to the highest level grid, with a partially converged solution obtained on each level. The procedure then reverses itself and the value of the dependent variables and the residuals are then transmitted to each successive coarser level, modified source terms generated, and a modified variable field obtained using the modified source term in place of the actual source term in the difference equations. Once the coarsest level is reached a variable correction is formed and is successively passed down to the finest grid. A new variable field on the finest grid is calculated in an iterative manner until the rate of convergence becomes nearly constant. If the solution has not converged to some specified limit the transfer of information to the coarser levels, previously described, is repeated. The calculations are continued in the cyclic manner described, until a converged solution is reached on the finest grid pattern.

In any flow field, regions of high spatial gradients of the dependent variable exist. In order to improve the accuracy of the finite difference solution in these regions it is common practice to use a finer grid pattern. If a uniform fine grid pattern is used over the complete region, an inefficient computational procedure results since the finer grids are not really required in the region containing small spatial gradients. Recognition of this has led to the use of

fine grid embedment techniques where fine grids are used in some regions while coarser grids are used in others.

The principle of fine grid embedment has been combined with the multilevel method to form the multilevel-multigrid (MLMG) method. The local grid refinement is introduced only on the higher multilevel grids (finer grid patterns) and covers only the spatial regions of interest.

### Numerical results

The MLMG algorithm was used to predict the mean vertical velocity profiles for the experimental test conditions. The grid structure used is shown in Fig 5. Six levels of grid refinement were used with the finest grid patterns,  $\Delta y = 1/256$ , used in the corner sections at the top

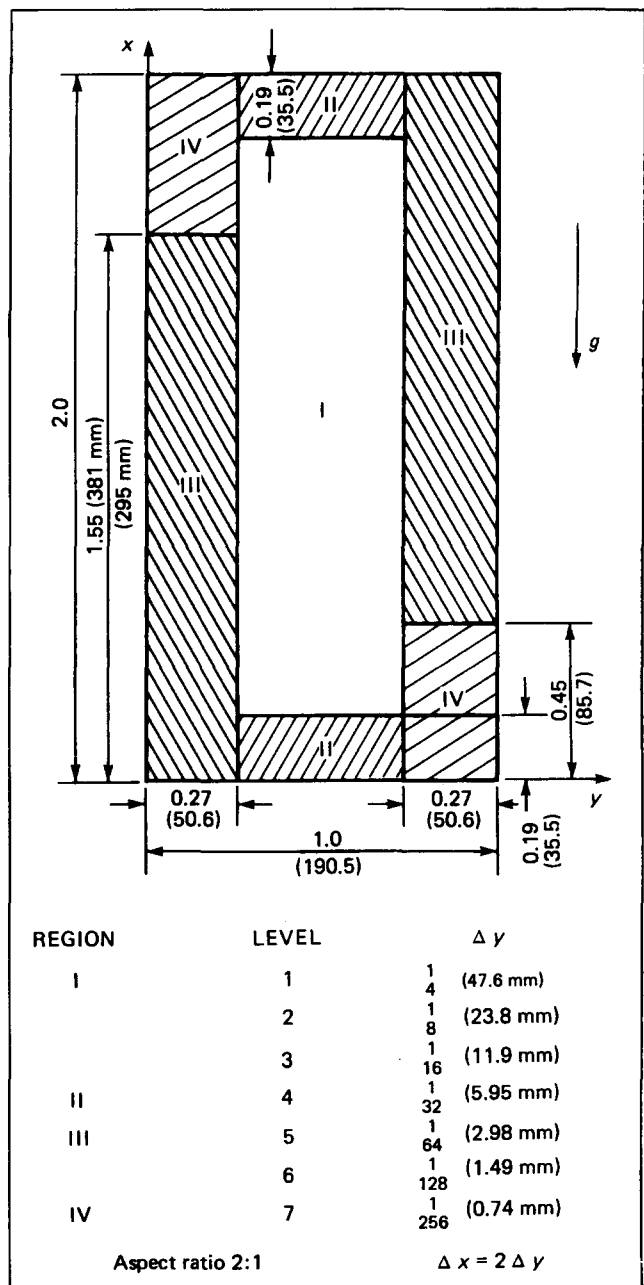


Fig 5 Multilevel-multigrid topology for prediction of flow

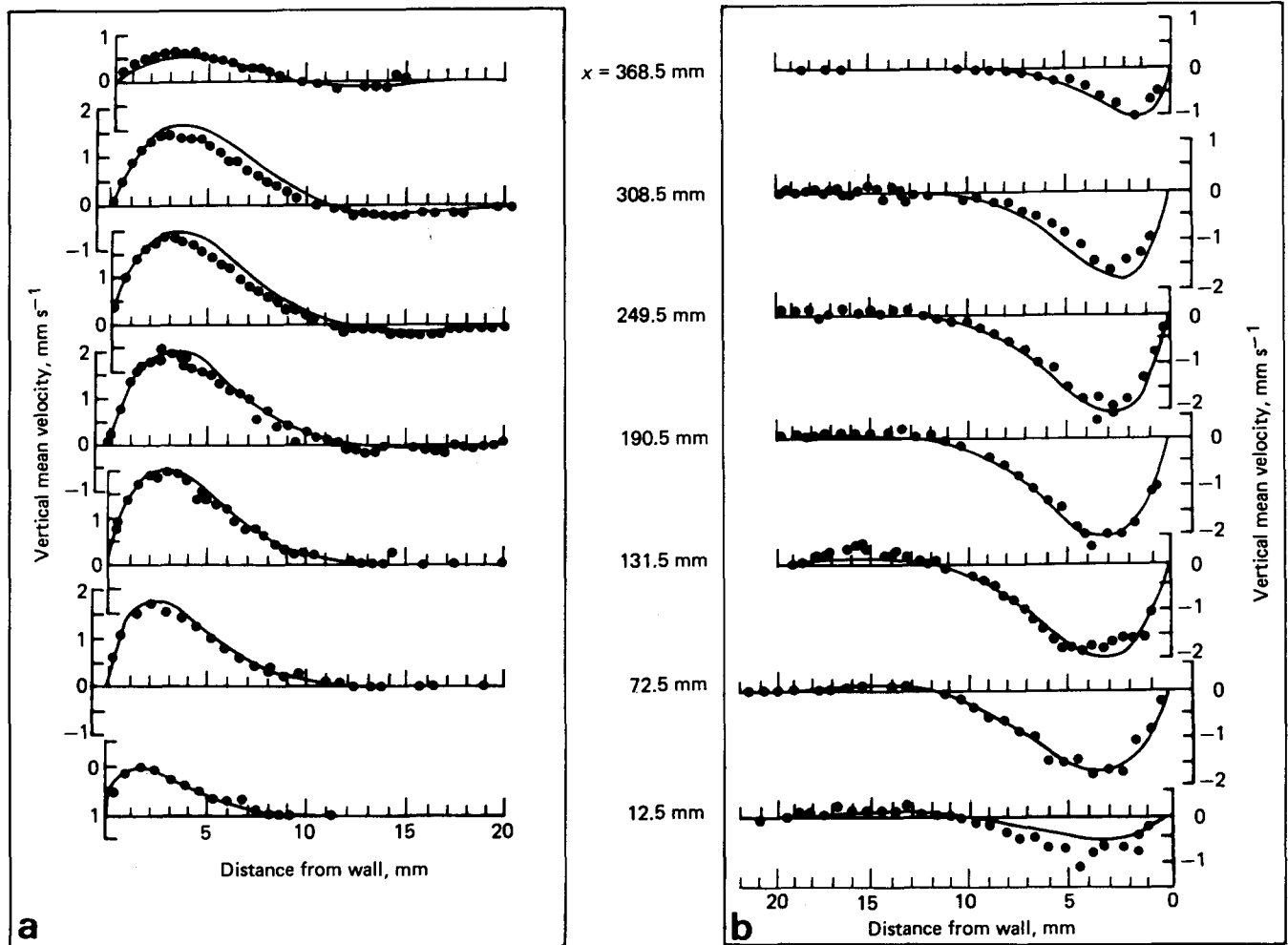


Fig 6 Comparison of predicted and experimental results: (a) hot wall; (b) cold wall

of the hot wall and the bottom of the cold wall. The aspect ratio of the grid pattern was 2:  $\Delta X = 2\Delta Y$ .

Both the predicted and experimental results are shown in Fig 6. The agreement is excellent and the calculations correctly predict the peak vertical velocities and the secondary recirculation.

### Conclusions

An experimental study of a natural convection laminar flow in a water-filled cavity with a 2:1 aspect ratio was conducted. The primary flow moved up the hot wall, across the top of the enclosure to the cold wall, down the cold wall and across the enclosure to the hot wall. Regions of secondary flow were found along the upper part of the hot wall and the lower part of the cold wall. These secondary flow regions were located between the primary flow and the fluid in the centre of the cell. The centre core is quiescent with a uniform horizontal temperature profile. The fluid in the core is stratified with a nearly uniform vertical temperature profile with a slope of  $4.42^\circ\text{C/m}$ .

A MLMG algorithm has been developed which accurately predicts the mean flow characteristics for the experimental test conditions.

### Acknowledgements

This work was supported under NSF Grant Number MEA-8025162, monitored by Dr Win Aung.

### References

1. Ostrach S. Natural convection in enclosures in *Advances in Heat Transfer*, Vol. 8, Academic Press, New York, 1972, 161-227
2. Catton I. Natural convection in enclosures. *Proc. 6th Int. Heat Transfer Conf.*, 1978, 2, 305-310
3. Ostrach S. Natural convection heat transfer in cavities and cells. *Proc. 7th Int. Heat Transfer Conf.*, 1982, 1, 365-379
4. Elder J. W. Laminar free convection in a vertical slot. *J. Fluid Mech.*, 1965, 23(1), 77-98
5. Elder J. W. Turbulent free convection in a vertical slot. *J. Fluid Mech.*, 1965, 23(1), 99-111
6. Mordchelles-Regnier G. and Kaplan G. Visualization of natural convection on a plane wall and in a vertical gap by differential interferometry: transition and turbulent regimes. *Proc. 1963 Heat Transfer and Fluid Mech. Inst.*, 1963, 94-111
7. Jannot M. and Mazeas C. Etude experimentale de la convection naturelle dans des cellules rectangulaires verticales. *Int. J. Heat Mass Transfer*, 1973, 16, 81-100
8. Kutateladze S. S., Kudyashkin A. G. and Ivakin V. P. Turbulent natural convection on a vertical plate and in a vertical layer. *Int. J. Heat Mass Transfer*, 1972, 15, 193-202

9. **Kutateladze S. S., Ivakin V. P., Kudyashkin A. G. and Kekalov A. N.** Turbulent natural convection in a vertical layer. *High Temp.*, 1977, **15**, 458–464
10. **Kutateladze S. S., Ivakin V. P., Kudyashkin A. G. and Kekalov A. N.** Thermal convection. *Heat Transfer—Soviet Research*, 1978, **10**, 118–125
11. **Yin S. H., Wung T. Y. and Chen K.** Natural convection in an air layer enclosed within rectangular cavities. *Int. J. Heat Mass Transfer*, 1978, **21**, 307–315
12. **Morrison G. L. and Tran V. Q.** Laminar flow structure in vertical free convective cavities. *Int. J. Heat Mass Transfer*, 1978, **21**, 203–213
13. **Ozoe H., Ohmuro M., Mouri A., Mishima S., Sayama H. and Churchill S. W.** Laser Doppler measurements of the velocity along a heated vertical wall of a rectangular enclosure. *ASME Trans., J. Heat Transfer*, 1983, **105**, 782–788
14. **Cowan G. H., Lovegrove P. C. and Quarni G. L.** Turbulent natural convection heat transfer in vertical single water-filled cavities. *Proc. 7th Int. Heat Transfer Conf.*, 1982, **2**, 195–204
15. **de Vahl Davis G.** Natural convection of air in a square cavity: a bench mark solution. *Int. J. Numer. Methods Fluids*, 1983, **3**, 249–264
16. **Jones I. P. and Thompson C. P.** (eds) Numerical solutions for a comparison problem on natural convection in an enclosed cavity, *AERE-R9955, HMSO, 1981*
17. **Issa R. I.** Solution of the implicitly discretized fluid flow equation by operator splitting, personal communication, 1984
18. **Phillips R. E. and Schmidt F. W.** A multilevel-multigrid technique for recirculating flows. *Numer. Heat Transfer*, 1985, **8**, 573–594
19. **Brandt A.** Multi-level adaptive solutions to boundary value problems. *Math. Comp.*, 1977, **31**, 333–390



## Planning Cogeneration Systems

Dilip R. Limaye

This recent book provides a mass of practical information and guidelines for those involved in evaluating, planning or implementing cogeneration (combined heat and power) projects in industrial, commercial and domestic situations.

The fourteen chapters cover a range of topics, including feasibility assessment, analytical methods for technical and economic feasibility evaluation, computerized system design, cogeneration technologies and application considerations, plus non-conventional technologies (such as waste heat recovery and the use of refuse derived fuel).

Readers will find that the book has been written with the United States regulatory environment in mind.

Cogeneration represents a classic case of how changing economic conditions can give an old technology new life. It has been practised since the turn of the century, but had declined steadily in importance in the USA for several decades. However, the events of the 1970s placed energy efficiency in a new, favourable light and led to a great resurgence of interest. This interest can be appreciated when we read that nearly half the primary energy consumed by US industry and electricity producers is lost as waste heat, totalling over seven million barrels per day of oil equivalent.

Throughout the text there are frequent references to the Public Utility Regulatory Policies Act (PURPA) and the National Energy Act of 1978 which removed many of the institutional and financial barriers to cogeneration. These Acts and other legislation appear to have opened the door to numerous cooperative ventures between industry and local electricity utilities.

One paper examines the potential for fuel cell-based cogeneration. This will continue a growing trend in small-scale prepackaged cogeneration systems.

Reducing the size at which cogeneration becomes economic will mean that these systems will exponentially expand the number of potential sites. Prospective new consumers will include anyone with a demand for both power and heat, such as hospitals, educational establishments, shopping centres, high-density housing developments and small industry. One author thought that more than 10,000 MW of new small cogeneration capacity could be installed in the next decade. These new small-scale, independent electricity producers could have a profound effect on the electricity industry of the USA and ultimately other countries.

Cogeneration will almost certainly continue to increase in importance in the coming years because of both the economic arguments (mainly the high cost of electricity) and the energy conservation potential.

Despite the fact that this book was produced for the USA market (with appropriate examples and non-SI units) it should prove to be of great value to those who are interested in this important field.

Andrew W. Cox  
University of Newcastle upon Tyne,  
Department of Chemical Engineering,  
Newcastle upon Tyne,  
UK

---

Published, by the Fairmont Press, Atlanta, USA, 246 pp.